Supplementary Material

Atomically tunable photo-assisted electrochemical oxidation process design for the decoration of ultimate-thin CuO on Cu_2O photocathodes and their enhanced photoelectrochemical performances

Dong Su Kim[a,1], Young Been Kim[a,1], Sung Hyeon Jung[a], Nishad G. Deshpande[a], Ji Hoon Choi[a], Ho Seong Lee[b], and Hyung Koun Cho[a,*]

[a] School of Advanced Materials Science and Engineering, Sungkyunkwan University, 2066, Seobu-ro, Jangan-gu, Suwon-si, Gyeonggi-do, 16419, Republic of Korea

[b] School of Materials Science and Engineering, Kyungpook National University, 80, Daehak-ro, Buk-gu, Daegu 41566, Republic of Korea

[1] Dong Su Kim and Young Been Kim contributed equally to this work.

* Corresponding author. Tel.: +82 31 290 7364; Fax: +82 31 290 7410; e-mail: chohk@skku.edu

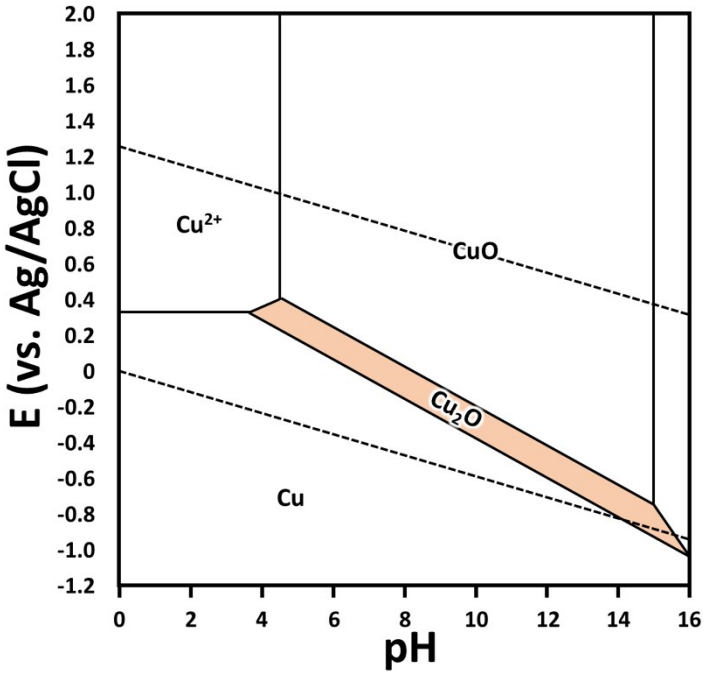

Figure S1. Pourbaix diagram of basic Cu metal elements including Cu_2O and CuO.

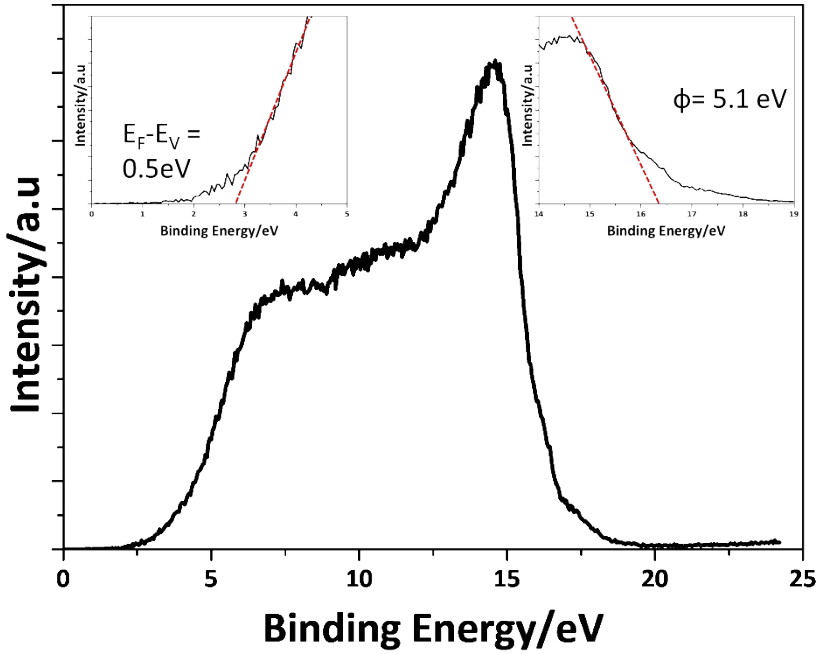

Figure S2. UPS spectrum using He I excitation for the work-function and valence band offset measurements of a Cu_2O:Sb/Cu_2O double layer.

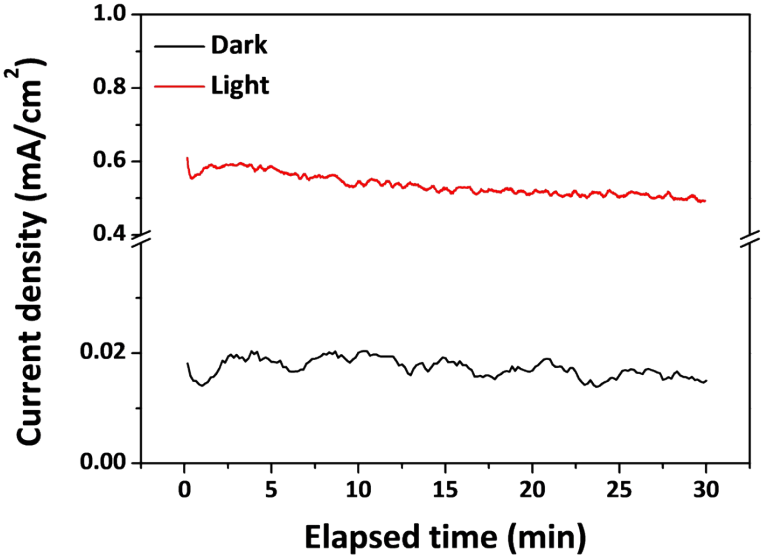

Figure S3. Current density–time transient curves showing the effect of light illumination on electrochemical oxidation reaction of the Cu_2O.

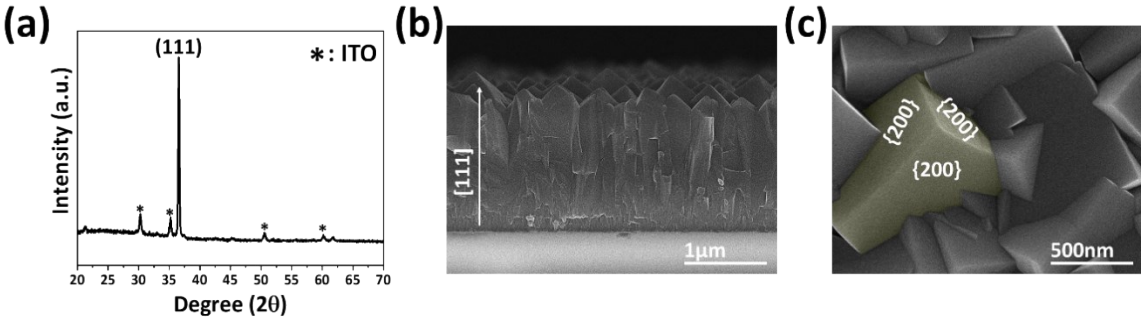

Figure S4. (a) XRD data of a Cu_2O absorber with the (111) prepared direction. SEM images of a Cu_2O absorber; (b) cross-section and (c) plan-view exposing the {200} triangular pyramid.

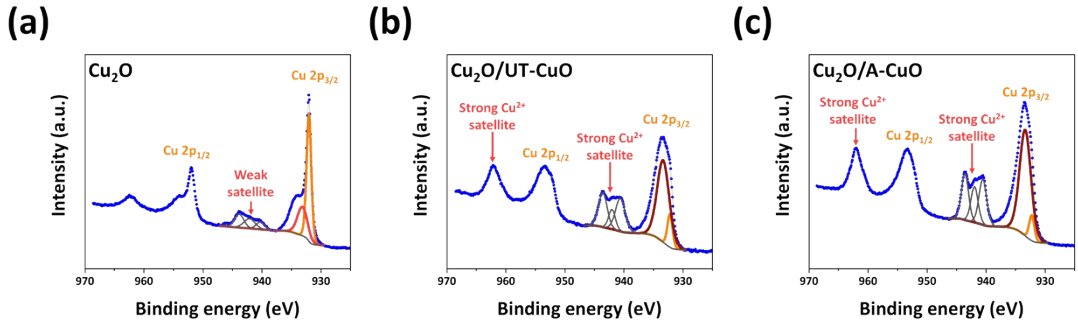

Figure S5. High resolution XPS spectra of (a) Cu_2O, (b) Cu_2O/UT-CuO, and (c) Cu_2O/A-CuO

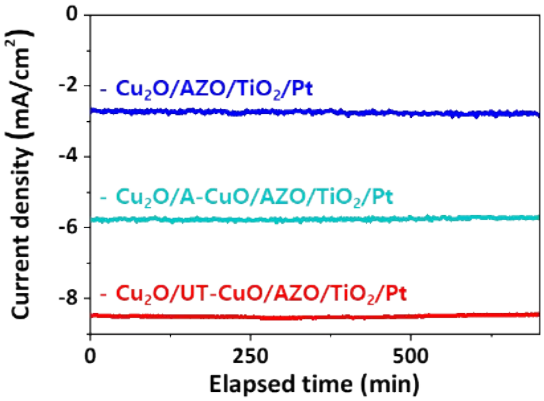

Figure S6. Stability test for $Cu_2O/AZO/TiO_2/Pt$, $Cu_2O/A\text{-}CuO/AZO/TiO_2/Pt$, and $Cu_2O/UT\text{-}CuO/AZO/TiO_2/Pt$ photocathodes at a fixed bias of 0 V versus RHE under continuous stirring.

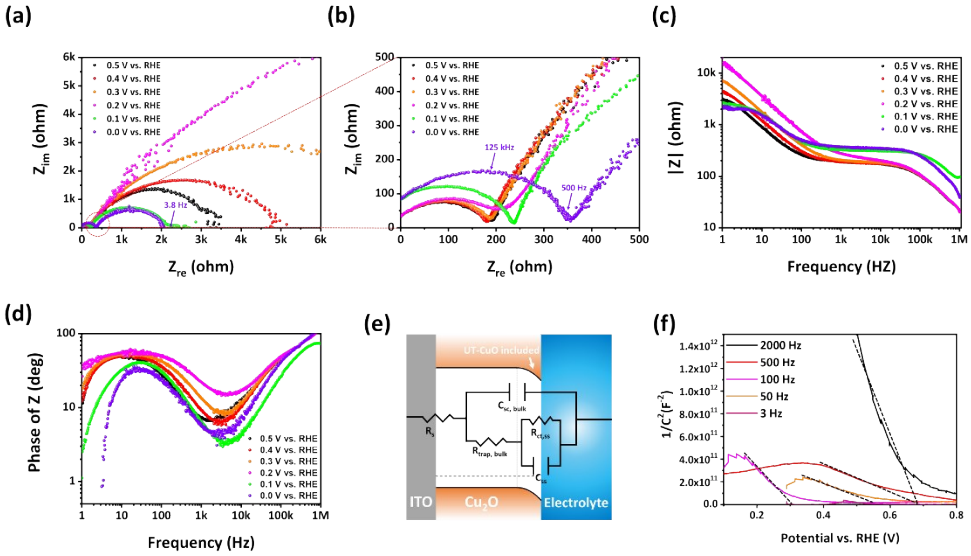

Figure S7. ITO/Cu_2O/UT-CuO/electrolyte structure: (a-b) Nyquist plots for various applied voltages from 0.5 V to 0 V vs. RHE, (c) Bode modulus plots, (d) Bode phase plots, and (e) the equivalent circuit. Here, R_s is involved with a series resistance between ITO and the Cu_2O layer and the conductivity of the electrolyte. The resistance $R_{trap,bulk}$ demonstrates accumulation and trapping of charges in the bulk of the Cu_2O layer. Also, $R_{ct,ss}$ indicates the resistance of charge transfer between the surface states of the photocathode and the electrolyte. The capacitances $C_{sc,bulk}$ and C_{ss} are related to the space charge capacitance of the bulk including UT-CuO and the surface state capacitance of the Cu_2O/electrolyte, respectively. (f) Mott–Schottky (MS) plots with respect to frequency.

In order to construct a rational equivalent circuit of the Cu_2O:Sb/Cu_2O/UT CuO/electrolyte structure, the impedance changes with an AC signal of 10 mV and a frequency range of 1 Hz to 1000 kHz at various applied voltages (0.5 – 0 V vs. RHE) were derived via Nyquist plots (Fig. S7 a-b). It is useful to understand the equivalent circuits under different band bending of the photoabsorbers by applying various voltages in the dark state. The formation of two semicircles was confirmed in the Nyquist plots. The first semicircle indicates the increase in capacitance with increase in applied voltage, resulting in the expansion of the C_{sc} contribution because the space charge region of the Cu_2O photoabsorber containing UT-CuO becomes larger. Cu_2O and UT-CuO form p-p junctions; therefore, the increase in capacitance due to the additional built-in potential is relatively negligible. The second semicircle C_{ss} is formed in the Cu_2O/electrolyte.[1, 2, 3] It is confirmed that $R_{ct,ss}$ and C_{ss} decreased at 0 V vs. RHE (HER state), which is a high applied voltage (Fig. S7 a). In the Mott–Schottky measurements, the space charge capacitance (C_{sc}) of the semiconductor can be evaluated with various applied potentials. C_{sc} can be determined from the fitting of the Nyquist plot or can be measured in the frequency range where only C_{sc} is affected with respect to the potential. As a result, the existence of the C_{sc} region is confirmed above 500 Hz, and the C_{ss} region is observed at the subsequent lower frequencies. Therefore, the frequency suitable for measuring the M–S plot in our sample is over 500 Hz; the flat band potential remains the same above 500 Hz and is not constant in the lower frequency range (Fig. S7 f).

References

1. W. Choi, H. C. Shin, J. M. Kim, J. Y. Choi and W. S. Yoon, *J. Electrochem. Sci. Technol.*, 2020, **11**, 1–13.

2. G. M. Kumar, F. Xiao, P. Ilanchezhiyan, S. Yuldashev and T. W. Kang, *RSC Adv.*, 2016, **6**, 99631–99637.

3. L. Contreras-Bernal, S. Ramos-Terrón, A. Riquelme, P. P. Boix, J. Idígoras, I. Mora-Seró and J. A. Anta, *J. Mater. Chem. A*, 2019, **7**, 12191–12200.

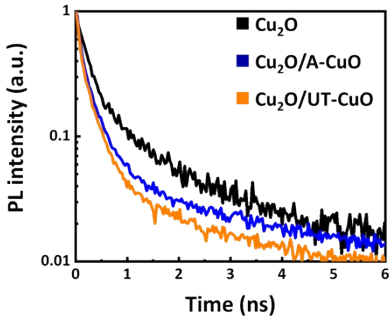

Figure S8. Time-resolved photoluminescence emission decay spectra of Cu_2O with three different surface conditions.

In TR-PL analysis (excited at 470 nm), the radiative and nonradiative recombination lifetimes of photoexcited electrons and holes can be determined by measuring the luminescence signals resulting from recombination. Fig. S8 shows the TR-PL results of our Cu_2O photocathode with and without CuO, in which all spectra were fitted with a biexponential function with the short (τ_S) and long (τ_L) lifetime components, as described in the previous TR-PL studies on semiconductor nanomaterials.[1,2]

Table S1. TRPL fitting data with a bi-exponential fitting model for various photocathodes.

Sample	Short life time (τ_s) ns	Long life time (τ_L) ns
Cu_2O	0.36	5.9
Cu_2O/A-CuO	0.33	3.2
Cu_2O/UT-CuO	0.29	2.6

As shown in Table S1, similar values of τ_S (0.36−0.29 ns) are obtained regardless of the samples, whereas τ_L largely decreases from 5.9 to 2.6 ns as the UT-CuO is inserted. The origin of τ_S can be attributed to non-radiative decay due to trap states, which is relatively irrelevant to the presence of the contact layer. However, τ_L is related to the time for the radiative interband recombination that decreases if the photogenerated charges are extracted to the contact layer. The smaller τ_L value for the ITO/Cu_2O/UT-CuO sample (2.6 ns) than that for the ITO/Cu_2O (5.9 ns) is indicative of the more-efficient photogenerated electron extraction through the CuO layer. This observation is supported by the fact that the PEC performance of Cu_2O photocathodes without a CuO layer is much lower than that with a CuO layer (Fig. S8). Hence, the coupling between Cu_2O and CuO film has resulted into enhanced charge transfer kinetics that helps in the enhancement of the photocurrent densities.[1, 2, 3]

References

1. W. Yang, S. Lee, H. C. Kwon, J. Tan, H. Lee, J. Park, Y. Oh, H. Choi and J. Moon, *ACS Nano*, 2018, **12**, 11088–11097.

2. N. Zhu, K. Zheng, K. J. Karki, M. Abdellah, Q. Zhu, S. Carlson, D. Haase, K. Žídek, J. Ulstrup, S. E. Canton, T. Pullerits and Q. Chi, *Sci. Rep.*, 2015, **5**, 1–14.
3. M. K. Son, L. Steier, M. Schreier, M. T. Mayer, J. Luo and M. Grätzel, *Energy Environ. Sci.*, 2017, **10**, 912–918.

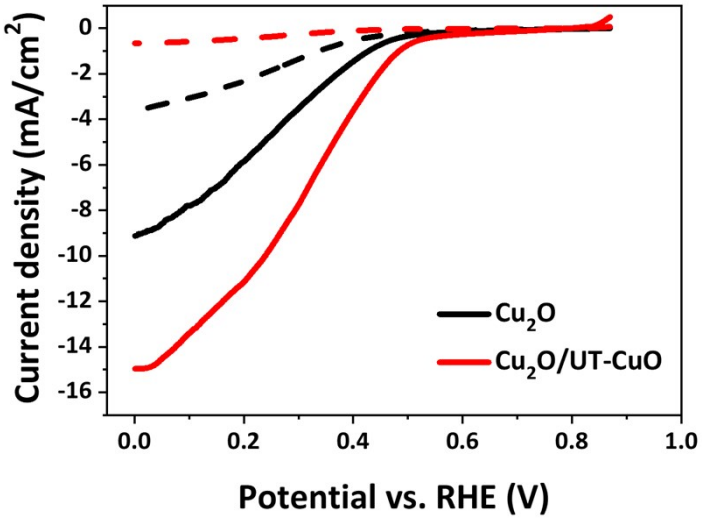

Figure S9. J–V response under simulated one-sun 1.5 G chopped illumination for Cu_2O and Cu_2O/UT-CuO photocathodes with scavenger.